Electronic supplementary information

Polypyrrole-polyaniline copolymer coated green rice husk ash as effective adsorbent for the removal of hexavalent chromium from contaminated water

Soumi Dutta,[a] Suneel Kumar Srivastava,[b]* Ashok Kumar Gupta [c]*

[a]School of Water Resources, Indian Institute of Technology Kharagpur, Kharagpur, West Bengal–721302, India

[b]Department of Chemistry, Indian Institute of Technology Kharagpur, Kharagpur, West Bengal–721302, India

[c]Department of Civil Engineering, Indian Institute of Technology Kharagpur, Kharagpur, West Bengal–721302, India

* **Corresponding author:**

S. K. Srivastava (Email: sunit@chem.iitkgp.ac.in)

A. K. Gupta (Email: agupta@civil.iitkgp.ac.in)

Contents

Materials and reagents

Analytical grade chemicals and reagents were used in this study. Pyrrole monomer (C_4H_4NH), aniline monomers ($C_6H_5NH_2$), ammonium persulfate (APS) ($(NH_4)_2S_2O_8$), potassium dichromate ($K_2Cr_2O_7$), ammonia solution (NH_3), hydrochloric acid (HCl), and sulfuric acid (H_2SO_4), were obtained from Merck Pvt. Ltd. India. All reagents were prepared using double distilled (DI) water. The stock solution of 1000 mg L^{-1} Cr(VI) was prepared by dissolving 2.8289 g of $K_2Cr_2O_7$ in 1000 ml of DI water. The desired concentrations of Cr(VI) were obtained by successive dilution of the stock solution. The raw rice hush in our work was collected from the local rice mill.

Characterization technique

The morphology of the polypyrrole, polyaniline, rice husk ash, and polypyrrole-polyaniline@rice husk ash (PPY-PANI@RHA) composite was analyzed by high-resolution Field Emission Scanning Electron Microscopy (FE-SEM) on Carl Zeiss Supra 40 instruments at an accelerating voltage of 20 kV. High-Resolution Transmission Electron Microscopy (HR-TEM) of the samples was investigated using Phillips CM 200 (Netherland) through an acceleration voltage of 200 kV. Fourier-transform infrared spectroscopy (FTIR) and Brunauer-Emmett-Teller (BET) surface area of the material was analyzed by using Perkin Elmer and Quanta chrome Autosorb IQ instruments, respectively. X-ray diffraction (XRD) pattern was used to analyze the crystalline phase of the material by recorded with D8 advance diffract meter, Bruker, Germany, with Cu K_α radiation (λ=0.154 nm) with a scanning rate of $2\theta=3^0$ per min. The zeta (ζ) potential of PPY-PANI@RHA adsorbent at different pH levels was measured by the Malvern Zetasizer Nano ZS DLS instrument.

The pH of the sample solution was measured by using glass electrode pH meter instruments from the ANALAB SCIENTIFIC pH/ORP Analyzer. Speed and temperature-controlled BOD incubator shaker were used for accompanying the adsorption experiments. Various physicochemical parameters of the collected wastewater sample were measured by following American Public Health Association (APHA) standard methods and using the multiparameter water quality meter (YSI 15M102692).

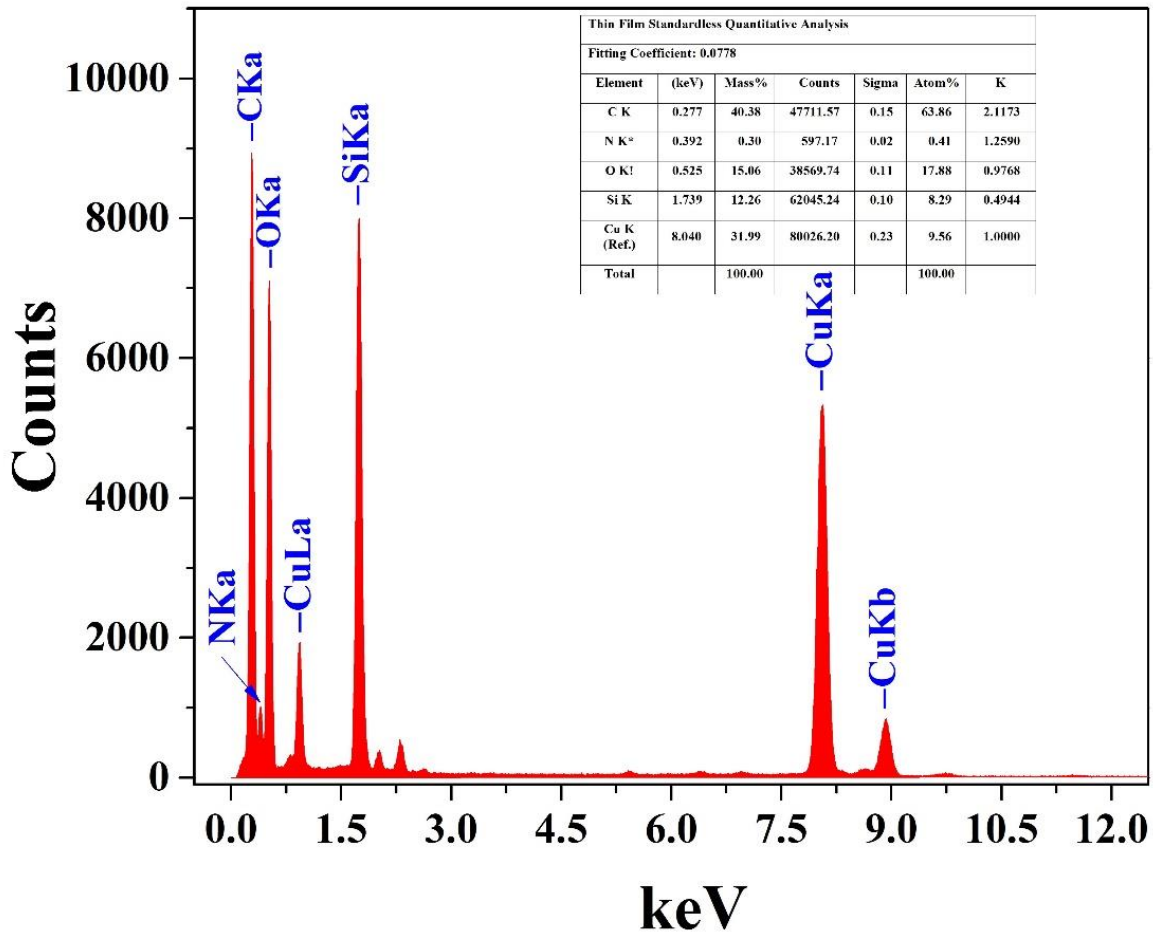

Fig. S1 Thin-film standardless quantitative analysis of PPY-PANI@RHA inferred from TEM analysis

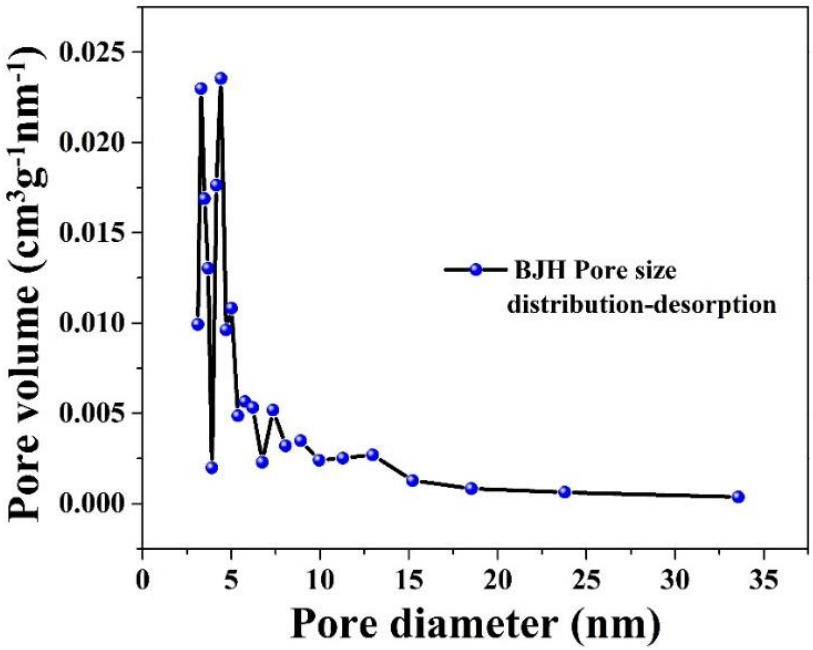

Fig. S2 BJH pore size distribution plot of PPY-PANI@RHA

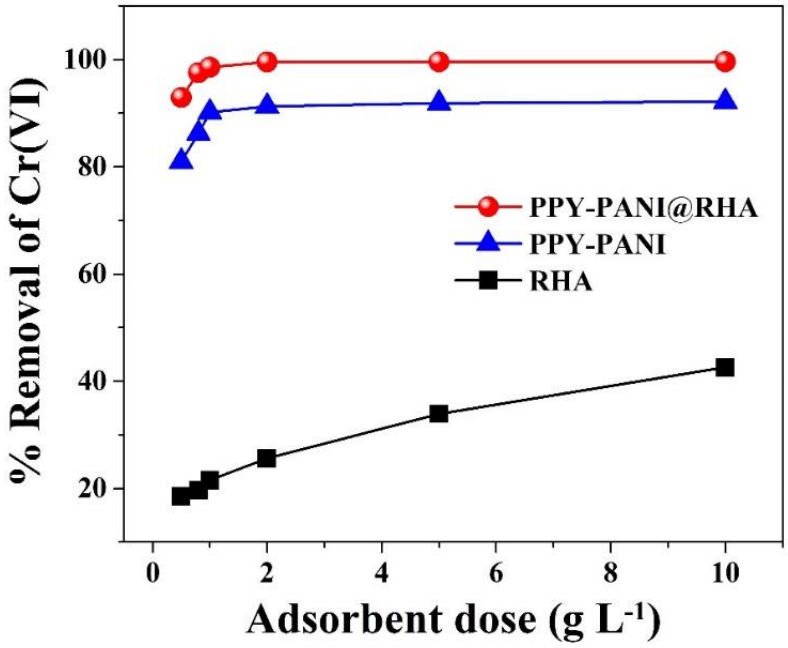

Fig. S3 The comparative study of Cr(VI) removal percentages using PPY-PANI@RHA, PPY-PANI, and RHA as adsorbent at different doses (Initial Cr(VI) concentrations: 50 mg L^{-1}; contact time: 300 min; agitation speed: 200 rpm; pH~2; temperature: 303K)

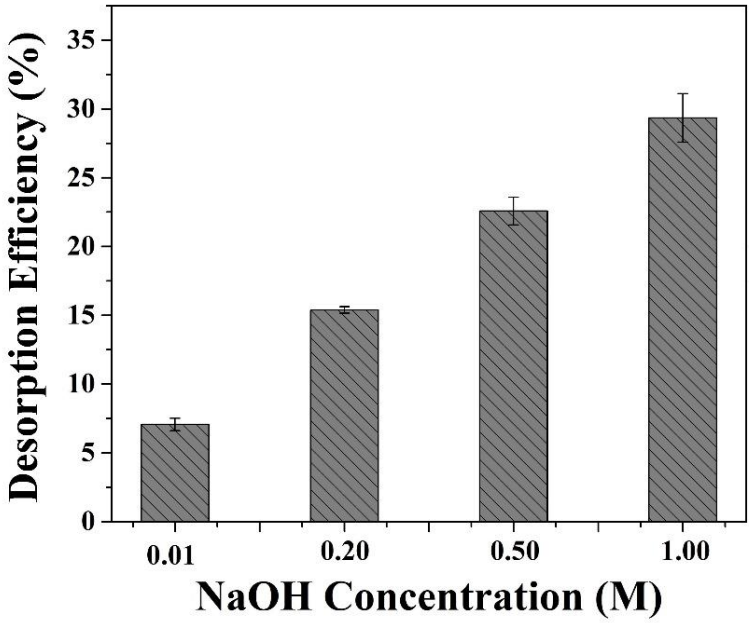

Fig. S4 Desorption efficiency of Cr(VI) ion from the surface of the PPY-PANI@RHA nanocomposites at different concentrations of NaOH (Agitation speed: 200 rpm; temperature: 303 K)

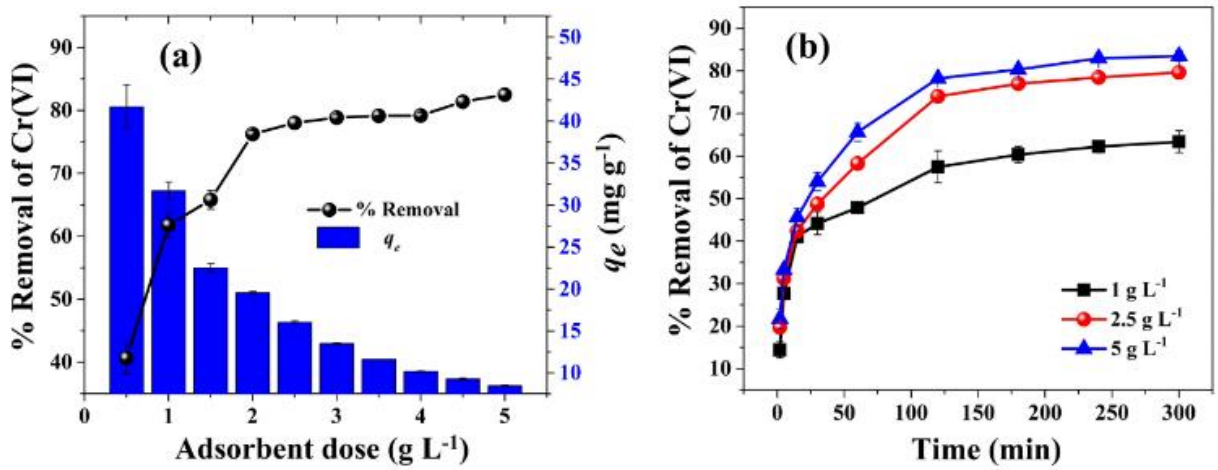

Fig. S5 (a) Effect of adsorbent dose on the Cr(VI) removal efficiency and Cr(VI) loading on PPY-PANI@RHA composites after reaching the equilibrium (Cr(VI) concentration of raw wastewater sample: 51.33 mg L^{-1}; contact time: 300 min; agitation speed: 200 rpm; temperature: 303 K), (b) Variation of % removal of Cr(VI) and adsorption capacity of PPY-PANI@RHA with contact time (Cr(VI) concentration of raw effluent sample: 51.33 mg L^{-1}; PPY-PANI@RHA dose: 0.8 g L^{-1}; temperature: 303 K, agitation speed: 200 rpm).

Table S1. Details of adsorption kinetics equations and parameters

Kinetics models	Equations	Parameters	References
Pseudo-first-order (PFO) model	$q_t = q_e(1 - e^{-k_1 t})$	q_t and q_e: (mg g^{-1}) adsorption capacity of the adsorbent at any time 't' and at equilibrium k_1: (min^{-1}) rate constant of the PFO equation	1
Pseudo-second-order (PSO) models	$q_t = \frac{(k_2\, q_e^2\, t)}{(1 + k_2 q_e\, t)}$	k_2: (g mg^{-1} min^{-1}) rate constant of the PSO equation	2
Elovich model	$q_t = \frac{1}{\beta} ln(1 + \alpha\beta t)$	α: (mg g^{-1} min^{-1}) initial sorption rate constant β: (g mg^{-1}) desorption constant	3
Intraparticle diffusion model	$q_t = k_d t^{0.5} + C$	k_d: (mg g^{-1} $min^{-0.5}$) rate constant of the intra-particle diffusion model C: (mg g^{-1}) constant associated with the thickness of the boundary layer	4
Boyd equation	$B_t = -0.4977 - \ln(1 - F)$	$F = q_t/q_e$, the fraction of solute adsorbed at different time 't' B_t: mathematical function of *'F'*	5

Table S2. Kinetic parameter values for Cr(VI) adsorption on PPY-PANI@RHA

Kinetic models		Parameters	50 mg L^{-1}	75 mg L^{-1}	100 mg L^{-1}
Pseudo-first-order model		q_e (mg g^{-1})	55.962	72.580	90.480
		k_1 (min^{-1})	0.371	0.399	0.473
		R^2	0.867	0.828	0.864
		Adj. R^2	0.857	0.814	0.852
		RMSE	6.299	9.490	10.180
Pseudo-second-order model		q_e (mg g^{-1})	57.826	75.097	93.051
		k_2 (g mg^{-1} min^{-1})	0.009	0.007	0.007
		R^2	0.932	0.893	0.918
		Adj. R^2	0.926	0.884	0.911
		RMSE	4.519	7.473	7.889
Elovich model		α (mg g^{-1} min^{-1})	4865.740	3986.940	30084.320
		β (g mg^{-1})	0.215	0.158	0.148
		R^2	0.996	0.991	0.994
		Adj. R^2	0.995	0.989	0.993
		RMSE	1.152	2.198	2.176
Intra-particle diffusion model	Steep slope	C (mg g^{-1})	37.347	48.675	65.828
		k_d (mg g^{-1} $min^{-0.5}$)	1.459	1.760	1.769
		R^2	0.957	0.979	0.947
		Adj. R^2	0.951	0.976	0.939
		RMSE	1.944	1.619	2.622
	Gradual slope	C (mg g^{-1})	59.972	65.662	81.747
		k_d (mg g^{-1} $min^{-0.5}$)	0.043	0.703	0.824
		R^2	0.830	0.982	0.915
		Adj. R^2	0.773	0.976	0.887
		RMSE	0.084	0.407	1.076
Boyd equation		R^2	0.988	0.981	0.899
		Adj. R^2	0.987	0.979	0.889

Table S3. Details of adsorption isotherm equations and parameters

Isotherm models	Equations	Parameters	References
Langmuir Isotherm	$q_e = \frac{q_{max}\, b\, C_e}{1 + b\, C_e}$	q_e: (mg g^{-1}) adsorption capacity of the adsorbent at equilibrium C_e: (mg L^{-1}) is the adsorbate concentration at equilibrium q_{max}: (mg g^{-1}) maximum saturated monolayer adsorption capacity of an adsorbent b: (L mg^{-1}) constant related to the affinity between an adsorbent and adsorbate	6
Freundlich Isotherm	$q_e = K_F\, C_e^{1/n}$	K_F: [(mg g^{-1})(L $mg^{-1})^{1/n}$] Freundlich adsorption capacity constant n: (dimensionless) Freundlich intensity parameter, which indicates the magnitude of the adsorption driving force or the surface heterogeneity	7
Dubinin-Radushkevich (D–R) Isotherm	$q_e = q_{DR} \exp(-K_{DR}\varepsilon^2)$	q_{DR}: (mg g^{-1}) adsorption capacity K_{DR}: D-R constant related to mean adsorption energy (mol^2 kJ^{-2}) ε: (Polanyi potential) = $RT ln[1 + \left(\frac{1}{C_e}\right)]$, where R is Gas constant (8.314 J mol^{-1} K^{-1}), and T is the absolute temperature (K)	8
Temkin Isotherm	$q_e = \frac{RT}{b_T} \ln(K_T C_e)$	K_T: Temkin isotherm constant b_T: Temkin constant related to the heat of sorption	9

Table S4. Isotherm parameter values of Cr(VI) adsorption on PPY-PANI@RHA

Isotherm models	Parameters	293 K	303 K	313 K
Langmuir Isotherm	q_{max} (mg g^{-1})	596.976	769.148	914.169
	b (L mg^{-1})	0.006	0.006	0.009
	R^2	0.962	0.964	0.980
	Adj. R^2	0.958	0.960	0.978
	RMSE	37.524	44.262	41.582
Freundlich Isotherm	K_F [(mg g^{-1})(L $mg^{-1})^{1/n}$]	31.107	36.946	51.045
	1/n	0.435	0.447	0.450
	R^2	0.997	0.995	0.999
	Adj. R^2	0.996	0.994	0.999
	RMSE	10.783	17.298	10.720
D–R Isotherm	q_{DR} (mg g^{-1})	358.750	415.090	656.552
	K_{DR} (mol^2 kJ^{-2})	39.548	12.622	373.498
	R^2	0.746	0.711	0.881
	Adj. R^2	0.714	0.675	0.866
	RMSE	97.451	125.809	101.677
Temkin Isotherm	K_T	3.120	35.471	30.087
	b_T	0.047	0.0565	0.045
	R^2	0.803	0.735	0.723
	Adj. R^2	0.778	0.701	0.689
	RMSE	85.890	120.627	154.749

Table S5. Comparisons of maximum adsorption capacity values of PPY-PANI@RHA with other reported polyaniline/polypyrrole based adsorbents for Cr(VI) remediation at 298±5 K

Type of adsorbent	Optimum pH	q_{max} (mg g^{-1})	References
PPy/Fe_3O_4/attapulgite	2.0	43.48	10
Sodium alginate-polyaniline nanofibers	2.0	73.34	11
Polypyrrole-Modified Layered Double Hydroxides (Mg-Al)	2.0	76.21	12
Chitosan/polypyrrole composite	4.2	78.61	13
Polyaniline Doped with Sulfuric Acid	2.0	95.79	14
Polyaniline/montmorillonite nanocomposites	2.0	167.50	15
PPy/Fe_3O_4 nanocomposite	2.0	169.50	16
Nanostructured polyaniline (PANI-HCl)	4.0	182.00	17
Fe_3O_4/PANI microspheres	2.0	200.00	18
Polypyrrole-polyaniline nano fibers	2.0	227.20	19
PPy/PANI composite films	2.0	256.41	20
Magnetic arginine-functionalized polypyrrole (Fe_3O_4@Arg-PPy)	2.0	322.58	21
Polypyrrole wrapped oxidized MWCNTs nanocomposites	2.0	294.10	22
PMMA/(rice husk ash)/polypyrrole membranes	2.0	371.74	23
Graphene/SiO_2@polypyrrole	2.0	429.20	24
Polyaniline@$Ni(OH)_2$	2.0	625.00	25
Polypyrrole/calcium rectorite composite	2.0	714.29	26
Polypyrrole/Polyaniline@Rice Hush Ash	2.0	769.15	**Present study**

Table S6. Thermodynamics parameters for Cr(VI) uptake by PPY-PANI@RHA nanocomposites

Temperature (K)	ΔG^0 (kJ mol^{-1})	ΔH^0 (kJ mol^{-1})	ΔS^0 (kJ mol^{-1} K^{-1})
293	-6.68	47.525	0.185
303	-8.53		
313	-10.38		

Table S7: Physicochemical parameters of the collected wastewater sample from CETP

Parameters	Values
Temperature (^{o}C)	25.8
pH	7.54
Total suspended solids (mg L^{-1})	2396
Total dissolved solids (mg L^{-1})	6888
Dissolved oxygen (mg L^{-1})	4.14
Specific Conductance (micro-siemens cm^{-1})	10664
Salinity (PSU)	6.06
Oxidation-Reduction Potential (ORP) (mV)	-376.9
Biochemical oxygen demand (BOD_5) (mg L^{-1})	149.3
Chemical oxygen demand (COD) (mg L^{-1})	287.88
Acidity (mg L^{-1}, as $CaCO_3$)	130
Alkalinity (mg L^{-1}, as $CaCO_3$)	124
Sulphate ion (mg L^{-1})	66.833
Hexavalent chromium (mg L^{-1})	51.325

Reference

1 S. Lagergren, Sven Vetenskapsakad Handingarl, 1898, 24, 1–39.
2 Y.-S. Ho, PhD Thesis, University of Birmingham, 1995.
3 S. Roginsky and Y. B. Zeldovich, Acta Phys Chem USSR, 1934, 1, 554.
4 W. J. Weber and J. C. Morris, J. Sanit. Eng. Div., 1963, 89, 31–60.
5 G. Boyd, A. Adamson and L. Myers Jr, J. Am. Chem. Soc., 1947, 69, 2836–2848.
6 I. Langmuir, J. Am. Chem. Soc., 1918, 40, 1361–1403.
7 H. Freundlich and others, J Phys Chem, 1906, 57, 1100–1107.
8 M. Dubinin, in Dokl. Akad. Nauk. SSSR., 1947, vol. 55, pp. 327–329.
9 M. Tempkin and V. Pyzhev, Acta Phys Chim USSR, 1940, 12, 327.
10 W. Sun, W. Zhang, H. Li, Q. Su, P. Zhang and L. Chen, RSC Adv., 2020, 10, 8790–8799.
11 R. Karthik and S. Meenakshi, Int. J. Biol. Macromol., 2015, 72, 711–717.
12 S. Sahu, P. Kar, N. Bishoyi, L. Mallik and R. K. Patel, J. Chem. Eng. Data, 2019, 64, 4357–4368.
13 R. Karthik and S. Meenakshi, Desalination Water Treat., 2015, 56, 1587–1600.
14 R. Zhang, H. Ma and B. Wang, Ind. Eng. Chem. Res., 2010, 49, 9998–10004.
15 J. Chen, X. Hong, Y. Zhao, Y. Xia, D. Li and Q. Zhang, J. Mater. Sci., 2013, 48, 7708–7717.
16 M. Bhaumik, A. Maity, V. V. Srinivasu and M. S. Onyango, J. Hazard. Mater., 2011, 190, 381–390.
17 J. Wang, K. Zhang and L. Zhao, Chem. Eng. J., 2014, 239, 123–131.
18 X. Han, L. Gai, H. Jiang, L. Zhao, H. Liu and W. Zhang, Synth. Met., 2013, 171, 1–6.
19 M. Bhaumik, A. Maity, V. V. Srinivasu and M. S. Onyango, Chem. Eng. J., 2012, 181–182, 323–333.
20 V. D. Thao, B. L. Giang and T. V. Thu, RSC Adv., 2019, 9, 5445–5452.
21 M. Chigondo, H. K. Paumo, M. Bhaumik, K. Pillay and A. Maity, J. Mol. Liq., 2019, 275, 778–791.
22 M. Bhaumik, S. Agarwal, V. K. Gupta and A. Maity, J. Colloid Interface Sci., 2016, 470, 257–267.
23 H. D. da Rocha, E. S. Reis, G. P. Ratkovski, R. J. da Silva, F. D. S. Gorza, G. C. Pedro and C. P. de Melo, J. Taiwan Inst. Chem. Eng., 2020, 110, 8–20.
24 W. Fang, X. Jiang, H. Luo and J. Geng, Chemosphere, 2018, 197, 594–602.
25 M. Bhaumik, V. K. Gupta and A. Maity, J. Environ. Chem. Eng., 2018, 6, 2514–2527.
26 Y. Xu, J. Chen, R. Chen, P. Yu, S. Guo and X. Wang, Water Res., 2019, 160, 148–157.